Analysis of sphingolipids in human corneal fibroblasts from normal and keratoconus patients[S]

Hui Qi,[*,†] Shrestha Priyadarsini,[*,†] Sarah E. Nicholas,[*,†] Akhee Sarker-Nag,[*,†] Jeremy Allegood,[§] Charles E. Chalfant,[§,] Nawajes A. Mandal,[1,2,*,†,††,§§] and Dimitrios Karamichos[2,*,†,††,§§]**

Departments of Ophthalmology,* Physiology,[††] and Cell Biology,[§§] University of Oklahoma Health Sciences Center (OUHSC), Oklahoma City, OK 73104; Dean McGee Eye Institute,[†] Oklahoma City, OK 73104; Department of Biochemistry and Molecular Biology,[§] Virginia Commonwealth University School of Medicine, Richmond, VA 23249; and Research and Development,** Hunter Holmes McGuire Veterans Administration Medical Center, Richmond, VA 23249 and VCU Massey Cancer Center, VCU Institute of Molecular Medicine, and VCU Johnson Center, Virginia Commonwealth University, Richmond, VA 23298

Abstract **The pathophysiology of human keratoconus (KC), a bilateral progressive corneal disease leading to protrusion of the cornea, stromal thinning, and scarring, is not well-understood. In this study, we investigated a novel sphingolipid (SPL) signaling pathway through which KC may be regulated. Using human corneal fibroblasts (HCFs) and human KC cells (HKCs), we examined the SPL pathway modulation. Both cell types were stimulated by the three transforming growth factor (TGF)-β isoforms: TGF-β1 (T1), TGF-β2 (T2), and TGF-β3 (T3). All samples were analyzed using lipidomics and real-time PCR. Our data showed that HKCs have increased levels of signaling SPLs, ceramide (Cer), and sphingosine 1-phosphate (S1P). Treatment with T1 reversed the increase in Cer in HKCs and treatment with T3 reversed the increase in S1P. *S1P3* receptor mRNA levels were also significantly upregulated in HKCs, but were reduced to normal levels following T3 treatment. Furthermore, stimulation with Cer and S1P led to significant upregulation of fibrotic markers in HCFs, but not in HKCs. Additionally, stimulation with a Cer synthesis inhibitor (FTY720) led to significant downregulation of specific fibrotic markers in HKCs (TGF-β1, collagen type III, and α smooth muscle actin) without an effect on healthy HCFs, suggesting a causative role of Cer and S1P in fibrogenesis.** **Overall, this study suggests an association of the SPL signaling pathway in KC disease and its relation with the TGF-β pathway.**—Qi, H., S. Priyadarsini, S. E. Nicholas, A. Sarker-Nag, J. Allegood, C. E. Chalfant, N. A. Mandal, and D. Karamichos. **Analysis of sphingolipids in human corneal fibroblasts from normal and keratoconus patients.** ***J. Lipid Res.*** **2017.** 58: **636–648.**

Supplementary key words cornea • lipidomics • transforming growth factor-β

Keratoconus (KC) is a bilateral noninflammatory progressive corneal ectasia with a prevalence of 1 per 2,000 in the general population (1). KC has its onset at puberty and is progressive until the third or fourth decade when it usually stops (2). There are three main characteristics to KC disease: corneal thinning, corneal bulging, and corneal scarring (3, 4). Vision deteriorates as the disease progresses and can lead to significant vision impairment at later stages. Clinically, early signs include oil droplets and corneal thinning. Over time, more significant signs appear, such as Vogt's stria, Fleisher's ring, and corneal scarring (5).

The available options to treat KC are contact lenses in early stages and hard contact lenses or hybrid lenses as the disease progresses. Intracorneal rings are used for mid-stage KC patients in order to improve the refractive error with no proven role in halting the progression of the disease. Eventually, once KC reaches advanced stages, corneal transplantation is required. Not every patient will get to that stage, but it is estimated that 20–25% of patients diagnosed with KC will reach the severe stage and undergo transplantation (6, 7).

This work was supported by National Eye Institute Grants EY025256, EY022071, EY023568, EY020886, and EY021725. Additional support was provided by research grants from the Veteran's Administration [VA Merit Review I BX001792 and RCS Award 13F-RCS-002 (C.E.C.)] and National Institutes of Health Grant HL125353 (C.E.C.). Services (Virginia Commonwealth University Lipidomics/Metabolomics Core) and products in support of the study were generated, in part, by the Virginia Commonwealth University Massey Cancer Center with funding from National Institutes of Health Grant P30 CA016059. The contents of this manuscript do not represent the views of the Department of Veterans Affairs or the US Government. The content is solely the responsibility of the authors and does not necessarily represent the official views of the National Institutes of Health.

Manuscript received 15 February 2016 and in revised form 8 February 2017.

Published, JLR Papers in Press, February 10, 2017
DOI 10.1194/jlr.M067264

Abbreviations: *ASAH1*, acylsphingosine amido-hydrolase 1; aSMA, α-smooth muscle actin; Cer, ceramide; CerS, ceramide synthase; Dh-Sph, dihydro-sphingosine; ECM, extracellular matrix; HCF, human corneal fibroblast; HKC, human keratoconus cell; KC, keratoconus; MGC, monoglycosylceramide; *SMPD1*, SM phosphodiesterase 1; S1P, sphingosine 1-phosphate; S1P1–5, sphingosine 1-phosphate receptors 1–5; Sph, sphingosine; SPHK, sphingosine kinase; SPL, sphingolipid; Spt, serine-palmitoyl transferase; T1, TGF-β1 isoform; T2, TGF-β2 isoform; T3, TGF-β3 isoform; TGF, transforming growth factor; VitC, ascorbic acid (vitamin C).

[1] Present address of N. A. Mandal: Department of Ophthalmology, Hamilton Eye Institute, University of Tennessee Health Sciences Center, Memphis, TN 38163.

[2] To whom correspondence should be addressed,
e-mail: nmandal@uthsc.edu (N.A.M.); Dimitrios-Karamichos@ouhsc.edu (D.K.)

[S] The online version of this article (available at http://www.jlr.org) contains a supplement.

Although a significant number of studies have been carried out, the pathophysiology of KC is still unknown. It is generally accepted that KC is a multifactorial disease (3, 8). A variety of factors have been considered, including genetic and environmental factors; however, most of the studies have been proven inconclusive. In fact, multiple studies have rarely identified the same loci or gene as being related to KC. With the absence of an animal model, most of the in vivo studies concentrate on the tear film and serum analysis (9–13). One of the few recognized links to KC disease is the association of individuals with Down syndrome. About 15% of the individuals with Down syndrome exhibit KC disease (14).

Our group has previously shown that human corneal fibroblasts (HCFs), when stimulated with a stable form of ascorbic acid (VitC), assemble an extracellular matrix (ECM) that mimics the in vivo stroma with alternating layers of collagen fibrils (15, 16). When human KC cells (HKCs) were tested on the same in vitro system, we found severe dysfunctions, including upregulation of fibrotic markers, metabolic dysfunction, and inability to secrete ECM (17–19). One way to "rescue" these cellular and ECM dysfunctions is by stimulating with transforming growth factor (TGF)-β3, as previously shown by our group (18). The current study investigates for the first time, to our knowledge, the role of lipids and, especially, sphingolipids (SPLs) on HKCs and their response to the three main TGF-β isoforms [TGF-β1 (T1), TGF-β2 (T2), and TGF-β3 (T3)].

Lipids play a fundamental role in a variety of tissues with regard to their metabolism and disease state (20). SPLs, a class of minor lipids, gained significant attention in recent years for their role in various cellular mechanisms and molecular signaling. SPLs were originally identified as structural components of biological membranes. Bioactive SPLs, most notably sphingosine (Sph) 1-phosphate (S1P) and ceramide (Cer), are now recognized to be important mediators of many basic cellular processes, including, but not limited to, cell migration, survival, contraction, proliferation, gene expression, and cell-cell interactions (21–24). By virtue of their ability to regulate these processes, there has been substantial recent interest in the ability of SPLs, particularly S1P, to regulate tissue fibrosis in various organ systems. S1P exerts its cellular effects predominantly through interactions with a family of specific cell surface G protein-coupled receptors, labeled S1P1–5 (21, 25). It acts on several types of target cells and is engaged in the profibrotic inflammatory process and the fibrogenic process through multiple mechanisms, which include vascular permeability change, leukocyte infiltration, migration, and proliferation, and myofibroblast differentiation of fibroblasts (26–29). Many of these S1P actions are receptor subtype specific. In these actions, S1P has multiple cross-talks with other cytokines, particularly TGF-β, which is the major focus of this study.

Overall, our study suggests a novel pathway for the regulation of HKCs in vitro. These novel findings may improve our understanding of KC pathobiology and may contribute to the identification of new biological targets and therapeutic agents.

METHODS

Isolation and expansion of primary cells

As previously described, HCFs were isolated from human corneas from healthy patients without ocular disease (16). All samples were obtained from the National Disease Research Interchange, Philadelphia, PA (http://www.ndri.org/). HKCs were isolated from human corneas from anonymized patients undergoing corneal transplantation for KC at Aarhus University Hospital, Aarhus, Denmark, as previously described (19). The research adhered to the tenets of the Declaration of Helsinki.

Corneal stromal cells were isolated following the protocol previously described (16). Briefly, the corneal epithelium and endothelium were removed from the stroma by scraping with a razor blade. Corneal stromal tissues were cut into small pieces (2 × 2 mm) and placed into T25 culture flaks. MEM (ATCC, Manassas, VA) containing 10% FBS (Atlantic Biologicals, Lawrenceville, GA) and 1% antibiotic (Gibco® antibiotic-antimycotic; Life Technologies) was added to the explants for 30 min incubation at 37°C. Cells were passaged into T75 culture flasks upon 100% confluence after 1–2 weeks of cultivation at 37°C, 5% CO_2.

Cell authentication

HCFs and HKCs are routinely isolated, in our lab, from human cadavers and/or transplant corneal tissues, ensuring that they are of human origin. Patient history, medical records, and serology testing provided by the National Disease Research Interchange ensures that the human tissue used in this study adheres to our strict inclusion/exclusion criteria. Furthermore, the isolated cells are routinely tested for corneal markers, such as keratocan, α-smooth muscle actin (aSMA), collagen-I, and collagen-V, using a variety of techniques that include real-time PCR, Western blots, and immunofluorescence (17, 30, 31).

Assembly of 3D in vitro ECM and TGF-β

Both HCFs and HKCs were cultured on 6-well tissue culture plates and processed for quantitative (q)RT-PCR and lipidomics (9, 32). These cells (1×10^6 cells/well) were seeded and cultured in MEM 10% FBS medium stimulated with 0.5 mM 2-O-α-D-glucopyranosyl-L-ascorbic acid (VitC; American Custom Chemicals Corporation, San Diego, CA). Cells were further stimulated with one of the three TGF-β isoforms, T1, T2, or T3. All isoforms were used at 0.1 ng/ml concentration, as previously optimized (19, 33, 34). The cultures were grown for 4 weeks before further processing. Cultures without any growth factors served as the controls. Fresh medium was supplied to the cultures, with or without the TGF-β isoforms every other day for the whole duration of the experiment.

S1P, Cers, and FTY720 inhibitor

HCFs and HKCs were initially grown in MEM 10% FBS medium and further seeded in 6-well plates (1×10^6 cells/well) and cultured. Fingolimod (FTY720) inhibitor (catalog number S5002; Selleck Chemicals) was dissolved, as per the manufacturer's instructions, in DMSO. Five different conditions were tested: controls, control+vehicle (vehicle final concentration in the medium was 10 nM), 10 nM FTY720, 1 uM FTY720, and 10 uM FTY720. Cer (C-8 Cer) (Cayman Chemicals) was dissolved, per the manufacturer's instructions, in DMSO and two different concentrations of Cers were used for the experiment (10 and 100 nM). S1P (Avanti Polar Lipids; Alabaster, AL) stock solution was prepared at a concentration of 125 μM for each of the S1P treatments by dissolving the S1P powder in 4 mg/ml of BSA. Four different conditions were tested: controls, 5 μm S1P, 10 nM Cer, and 100 nM Cer. The medium was changed every other day for the duration of the

experiment. At the end of week 2, all constructs were processed for lipidomics, Western blot, and qRT-PCR analysis.

Real-time PCR

For evaluation of the mRNA expression, qRT-PCR was done on all samples, as previously described (35–39). Briefly, total RNA extraction was carried out using Ambion RNA mini extraction kit (Ambion TRIzol® Plus RNA purification kit**:** Life Technologies, Carlsbad, CA). The cDNA synthesis was followed by using SuperScript™ III First-Strand Synthesis SuperMix (Invitrogen, Carlsbad, CA) according to the manufacturer's protocol. Expression of SPL metabolic genes was assayed by SYBR Green methods. Primers for qRT-PCR were designed in such a way that they spanned at least one intron, which eliminated the chance of amplification from residual genomic DNA contamination. Sequences of the primers for major human SPL metabolic genes were custom synthesized and used for qRT-PCR. The genes and the primer sequences are as follows: acid ceramidase or acylsphingosine amido-hydrolase 1 (*ASAH1*) (forward, 5′-GAGTTGCGTCGCCTTAGT-3′; reverse, 5′-CATGGAACTGCACCTCTGTA-3′), acid sphingomyelinase or SM phosphodiesterase 1 (*SMPD1*) (forward, 5′-GAAGAGCTGGAGCTGGAATTA-3′; reverse, 5′-CTGGGTCAGATTCAGGATGTAG-3′), S1P receptor 2 (forward, 5′-GGCCTAGCCAGTTCTGAAAG-3′; reverse, 5′-TCCAGCGTCTCCTTGGTATAA-3′), Sph kinase (*SPHK*) *1* (forward, 5′-GGTGTGTGCAGAGGAGTTG-3′; reverse, 5′-CAGTCTGGCCGTTCCATTAG-3′), and *SPHK2* (forward, 5′-GTTGTGCTGAAGAGGTTGTTC-5′; reverse, 5′-CTGGTCAAAGGTGAGGATCTTA-3′). Quantitative PCR and melt-curve analyses were performed using iQ EvaGreen Supermix (Bio-Rad, Hercules, CA) and an iCycler machine. Relative quantities of expression of the genes of interest in different samples were calculated by the comparative Ct (threshold cycle) value method, as described earlier (35–40).

During this study, some of the TaqMan gene expression assay (Applied Biosystems) probes were also used. GAPDH (Hs99999905_m1) and 18S (Hs99999901_s1) were used as housekeeping genes/controls and TGF-β1 (Hs00998133_m1), ACTA2/SMA (Hs00426835_m1), and COL3A1 (Hs00943809_m1) were experimental probes. The reaction was set up using 10 ng of cDNA in a 20 μl reaction containing our probe of interest and TaqMan FaSt Advanced Master Mix (Applied Biosystems, Life Technologies). Sample amplification was made by the StepOnePlus real-time PCR system (Life Technologies) using manufacturer's standard protocol.

Western blots

Cell lysates were used for Western blot analysis, per our previously optimized protocol (41, 42). Preparation of cell lysates was initiated by using RIPA buffer [50 mM Tris (pH 8), 150 mM NaCl, 1% Triton X-100, 0.1% SDS, 1% sodium deoxycholate; Abcam, Cambridge, MA] containing protease and phosphatase inhibitors (Sigma-Aldrich, St. Louis, MO) followed by brief incubation, centrifugation, and storage at −20°C until needed. BCA assay (Thermo Scientific, IL) was initiated to identify total protein concentration and purity assessment. Equal amounts of proteins were loaded on a 4–20% Tris-glycine gel (Novex; Life Technologies) for gel electrophoresis; the proteins were transferred to a nitrocellulose membrane (Novex; Life Technologies); and the membrane was incubated in 5% BSA blocking solution (Thermo Scientific). The following primary antibodies were used: anti-collagen-III (ab7778; Abcam), anti-TGF β1 (ab53169; Abcam), anti-aSMA (ab5694; Abcam), and anti-GAPDH (ab9485; Abcam). Antibodies were used at a 1:1,000 dilution in TBST overnight at 4°C, followed by incubation with a secondary antibody (Alexa Flour® 568 donkey anti-rabbit IgG [H+L]; Abcam) at 1:2,000 dilution for 1 h. A UVP imaging system (Upland, CA) was used to detect bands and quantification by densitometry. Net intensities were normalized to the loading control (GAPDH) and are depicted as fold change.

Extraction and analysis of SPLs

SPLs were analyzed in the Lipidomics Core at Virginia Commonwealth University, Richmond, VA, following previously published protocols (43–46). Internal standards were purchased from Avanti Polar Lipids (Alabaster, AL). Internal standards were added to samples in 20 ul ethanol:methanol:water (7:2:1) as a cocktail of 500 pmol each. Standards for sphingoid bases and sphingoid base 1-phosphates were 17-carbon chain length analogs: C17-Sph, (2S,3R,4E)-2-aminoheptadec-4-ene-1,3-diol (d17:1-So); C17-sphinganine, (2S,3R)-2-aminoheptadecane-1,3-diol (d17:0-Sa); C17-S1P, heptadecasphing-4-enine-1-phosphate (d17:1-So1P); and C17-sphinganine 1-phosphate, heptadecasphinganine-1-phosphate (d17:0-Sa1P). Standards for N-acyl SPLs were C12-fatty acid analogs: C12-Cer, N-(dodecanoyl)-sphing-4-enine (d18:1/C12:0); C12-Cer 1-phosphate, N-(dodecanoyl)-sphing-4-enine-1-phosphate (d18:1/C12:0-Cer1P); C12-SM, N-(dodecanoyl)-sphing-4-enine-1-phosphocholine (d18:1/C12:0-SM); and C12-glucosylceramide, N-(dodecanoyl)-1-β-glucosyl-sphing-4-eine. The MS grade solvents [chloroform (EM-CX1050) and methanol (EM-MX0475), as well as formic acid (ACS grade, EM-FX0440-7)] were obtained from VWR (West Chester, PA).

For LC-MS/MS analyses, a Shimadzu LC-20 AD binary pump system coupled to a SIL-20AC autoinjector and DGU20A3 degasser coupled to an ABI 4000 quadrupole/linear ion trap (QTrap) (Applied Biosystems) operating in triple quadrupole mode was used. Q1 and Q3 were set to pass molecularly distinctive precursor and product ions (or a scan across multiple *m/z* in Q1 or Q3), using N2 to collisionally induce dissociations in Q2 (which was offset from Q1 by 30–120 eV); the ion source temperature set to 500°C.

Samples were collected into 13 × 100 mm borosilicate tubes with a Teflon-lined cap (catalog number 60827-453; VWR). Then, 1 ml of CH_3OH and 0.5 ml of $CHCl_3$ were added along with the internal standard cocktail (500 pmol of each species dissolved in a final total volume of 20 μl of ethanol:methanol:water 7:2:1). The contents were dispersed using an ultra sonicator at room temperature for 30 s. This single phase mixture was incubated at 48°C overnight. After cooling, 75 μl of 1 M KOH in CH_3OH were added and, after brief sonication, incubated in a shaking water bath for 2 h at 37°C to cleave potentially interfering glycerolipids. The extract was brought to neutral pH with 6 μl of glacial acetic acid, then the extract was centrifuged using a table-top centrifuge, and the supernatant was removed by a Pasteur pipette and transferred to a new tube. The extract was reduced to dryness using a SpeedVac. The dried residue was reconstituted in 0.5 ml of the starting mobile phase solvent for LC-MS/MS analysis, sonicated for ∼15 s, and then centrifuged for 5 min in a tabletop centrifuge before transfer of the clear supernatant to the autoinjector vial for analysis.

The sphingoid bases, sphingoid base 1-phosphates, and complex SPLs were separated by reverse phase LC using a Supelco 2.1 (internal diameter) × 50 mm Ascentis Express C18 column (Sigma-Aldrich) and a binary solvent system at a flow rate of 0.5 ml/min with a column oven set to 35°C. Prior to injection of the sample, the column was equilibrated for 0.5 min with a solvent mixture of 95% mobile phase A1 ($CH_3OH/H_2O/HCOOH$, 58/41/1, v/v/v, with 5 mM ammonium formate) and 5% mobile phase B1 ($CH_3OH/HCOOH$, 99/1, v/v, with 5 mM ammonium formate), and after sample injection (typically 40 μl), the A1/B1 ratio was maintained at 95/5 for 2.25 min, followed by a linear gradient to 100% B1 over 1.5 min, which was held at 100% B1 for 5.5 min, followed by a 0.5 min gradient return to 95/5 A1/B1. The column

was re-equilibrated with 95:5 A1/B1 for 0.5 min before the next run. The species of Cer, hexosyl-Cer, SM, and sphingoid lipids, such as Sph, dihydro-Sph (Dh-Sph), S1P, and Dh-S1P, were identified based on their retention time and *m/z* ratio and quantified as described in previous publications (45, 46). The detailed MS parameters and species identification chart are shown in **Table 1**.

Statistical analysis

Data analysis for the sample sets was done by one-way ANOVA using GraphPad Prism 6 software. $P < 0.05$ was considered to be statistically significant.

RESULTS

SPL profile of HCFs and HKCs

To our knowledge, no study has been done on the SPL composition of HCFs and HKCs. Herein, we determined the composition of major SPLs in cultured HCFs treated with VitC by LC-MS/MS. We found that 91% of the nonsialilated SPLs of HCFs belong to SMs, 8% to Cers, and 1% to monoglycosylceramides (MGCs) (glucosyl + galactosyl Cers) (**Fig. 1**). HKC SPL composition appears to be very similar to that of HCFs (Fig. 1). We then calculated the total absolute quantity of each SPL class and included to that analysis of the less abundant, but important for signaling, SPLs such as Sph, Dh-Sph, and S1P. Though there were no significant changes in the relative composition of the major classes of SPLs (Fig. 1), we found that the absolute quantity of Cer ($P < 0.001$; n = 4) and S1P ($P < 0.01$; n = 4) was significantly higher in HKCs (**Fig. 2**). **Table 2** shows the major species of Cers from both HCFs and HKCs, treated with VitC only (control) and three isoforms of TGF-β. In HCFs, C16:0 Cer accounts for the highest levels (42.6 mol%) followed by C24:1 Cer (22.0 mol%), C24:0 Cer (14.6 mol%), C22:0 Cer (7.9 mol%), and C18:0 Cer (6.1 mol%) (supplemental Table S1A; Table 2, HCF control). The species distribution of Cers in HKCs had a slightly different pattern: C16:0 Cer (34.0 mol%) followed by C24:1 Cer (22.4 mol%), C24:0 Cer (17.3 mol%), C18:0 Cer (9.8 mol%), and C22:0 Cer (9.4 mol%) (supplemental Table S1A; Table 2, HKC control). The absolute quantity of Cer individual species,

TABLE 1. AB Sciex 5500 QTrap mass spectrometer settings

	N-Acyl	Q1 (*m/z*)	Q3 (*m/z*)	Declustering Potential (V)	Collision Energy (V)	Collision Cell Exit Potential (V)
Long-chain bases	—					
d17:1 So	—	286.4	268.3	100	15	10
d17:0 Sa	—	288.4	270.4	100	21	9
d18:1 So	—	300.5	282.3	100	21	11
d18:0 Sa	—	302.5	284.3	100	21	10
d17:1 S1P	—	366.4	250.4	90	23	12
d17:0 Sa1P	—	368.4	252.4	90	23	12
d18:1 S1P	—	380.4	264.4	90	25	12
d18:0 Sa1P	—	382.4	266.4	90	25	12
Complex SPLs						
Cer	C12:0	482.6	264.4	60	35	10
	C14:0	510.7	264.4	60	36	10
	C16:0	538.7	264.4	60	37.5	10
	C18:1	564.7	264.4	60	39	10
	C18:0	566.7	264.4	60	39	10
	C20:0	594.7	264.4	60	40	10
	C22:0	622.8	264.4	60	41.5	10
	C24:1	648.9	264.4	60	42.5	10
	C24:0	650.9	264.4	60	42.5	10
	C26:1	676.9	264.4	60	45	10
	C26:0	678.9	264.4	60	45	10
MonoHexCer	C12:0	644.6	264.4	80	40	10
	C14:0	672.6	264.4	80	41.5	10
	C16:0	700.7	264.4	80	42.5	10
	C18:1	726.7	264.4	80	43.5	10
	C18:0	728.7	264.4	80	43.5	10
	C20:0	756.7	264.4	80	45	10
	C22:0	784.8	264.4	80	47	11
	C24:1	810.9	264.4	80	47.5	11
	C24:0	812.9	264.4	80	47.5	11
	C26:1	838.9	264.4	80	48	11
	C26:0	840.9	264.4	80	48	11
SM	C12:0	647.7	184.4	70	40	12
	C14:0	675.7	184.4	70	41	12
	C16:0	703.8	184.4	70	42.5	12
	C18:1	729.8	184.4	70	44	12
	C18:0	731.8	184.4	70	45	12
	C20:0	759.9	184.4	70	47	12
	C22:0	787.9	184.4	70	47.5	12
	C24:1	813.9	184.4	70	47.5	13
	C24:0	815.9	184.4	70	47.5	13
	C26:1	841.9	184.4	70	50	13
	C26:0	843.9	184.4	70	50	13

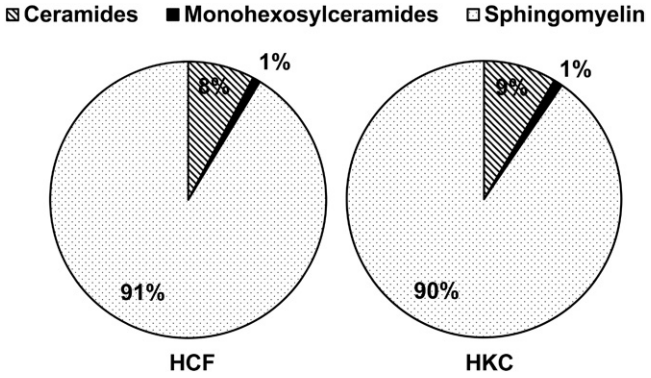

Fig. 1. SPL composition of cultured HCFs from normal and KC corneas. Major classes of SPLs such as Cers, monohexosyl (glycosyl + galactosyl) Cers, and SMs were analyzed with LC-MS/MS from primary culture of HCFs and HKCs.

such as C16:0 ($P < 0.05$), C20:0 ($P < 0.01$), C22:0 ($P < 0.05$), C24:1 ($P < 0.01$), and C24:0 ($P < 0.05$), was significantly higher in HKCs than in HCFs (Table 2).

The total MGCs and the relative composition of the major species of MGCs were not significantly different in control HKCs and control HCFs (Fig. 2, supplemental Table S1B). We further analyzed the composition of SM; the total SM level in HKCs was not different from HCFs (Fig. 2). The composition analysis of the major species suggests that, in HCFs, C16:0 SM accounts for the highest levels (41.0 mol%) followed by C24:1 SM (19.9 mol%), C18:0 SM (14.4 mol%), C24:0 SM (10.9 mol%), and C22:0 SM (8.5 mol%) (supplemental Table S1C; **Table 3**). Species distribution of SM in HKCs follows a similar pattern: C16:0 SM (37.0 mol%) followed by C24:1 SM (18.7 mol%), C18:0 SM (13.4 mol%), C24:0 SM (11.1 mol%), and C22:0 SM (9.6 mol%) (supplemental Table S1C). Most of the individual species of SM, as well as the total SM, appeared to be increased in HKCs; however, they were not found to be statistically significant, except C22:0 SM ($P < 0.05$) (Table 3).

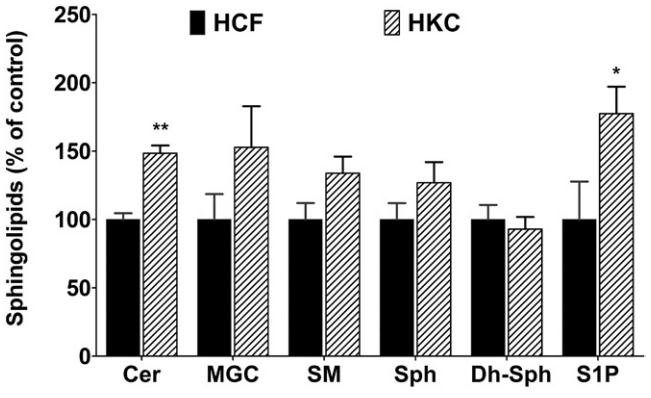

Fig. 2. SPL composition of cultured HCFs and HKCs. The total absolute quantity (picomoles per milligram of cells) of the major SPL species, such as Cers, MGCs, and SMs, and minor signaling SPLs, such as Sph, Dh-Sph, and S1P, were analyzed with LC-MS/MS and are presented here as the comparison of HCFs and HKCs, where HCFs are considered as control. *$P \leq 0.01$ (n = 4) and **$P \leq 0.001$ (n = 4) indicate the statistically significant difference between HCFs and HKCs.

SPL profile regulated by TGF-β isoforms

TGF-β is known to play a role in corneal wound healing as well as KC defects. We have previously studied the effects of TGF-β isoforms in HCFs and HKCs with regard to their effects on fibrosis, metabolism, and ECM assembly (17, 19, 31). Here, we investigated the effect of TGF-β isoforms on SPL composition in both HCFs and HKCs. In HCFs, we found that the T1 treatment significantly reduced the levels of all major SPL classes, such as Cer, MGC, SM, Sph, and Dh-Sph (**Fig. 3**, $P < 0.01$). However, T1 treatment did not affect the levels of S1P (Fig. 3). The T2 and T3 treatments, on the other hand, did not affect the total levels of any SPL class, except for Dh-Sph, where significant reduction was found by both T2 and T3 (Fig. 3; $P < 0.001$). In HKCs, T1 treatment reduced the levels of Cer and Dh-Cer, but none of the other SPLs (**Fig. 4**; $P < 0.01$). T2 treatment reduced all three minor lipids [Sph, Dh-Sph, and S1P ($P < 0.01$)] and T3 treatment reduced both Dh-Sph and S1P significantly ($P < 0.01$) (Fig. 4). Thus it appears that all the TGF-β isoforms have some effect on SPL profiles in HCFs and HKCs and there is a differential effect of each isoform in the two cell lines.

When we looked into the individual species, we found, very interestingly, that in HCFs the T1 treatment reduced both short- and long-chain Cers (C16:0, C20:0, C24:1) (Table 2; $P < 0.01$); however, the relative composition of these species remained the same (supplemental Table S1A). As reflected in the total Cer levels (Fig. 3), we did not see any changes in individual species of Cers in HCFs with the T2 and T3 treatments (Table 3). The relative composition of C16:0 and C24:0 appeared to be affected by T2 treatment in HCFs (supplemental Table S1A). In contrast, in HKCs, only C16 Cer was reduced significantly upon T1 treatment and there was no effect with the T2 and T3 treatments (Table 2; $P < 0.01$).

By analyzing the relative composition of the major species of MGCs in HCFs, we found that T2 treatment significantly increased the ratio of C24:1 and T3 treatment increased C16:0 (supplemental Table S1B; $P < 0.01$). The relative composition of the major MGC species in HKCs was not different from HCFs; however, the T1, T2, and T3 treatments decreased the relative level of C16:0 species in HKCs and the T1 and T3 treatments increased the levels of C24:1 MGC (supplemental Table S1B; $P < 0.01$).

In SMs, the T1 treatment downregulated the levels of long-chain Cers containing SM species (C24:0 and C24:1) (Table 3). In control HKCs, the levels of C22:0 were significantly higher than in HCFs; however, treatment with the TGF-β isoforms did not affect the levels of individual species of SM in HKCs (Table 3). As total Cer and total SM were higher in HKCs, many individual species were higher in HKCs when compared with similarly treated HCFs (Table 3; $P < 0.01$). The T2 treatment appeared to significantly reduce the relative composition of C16:0 in HCFs (supplemental Table S1C).

Expression of SPL metabolic genes

We further determined the expression of some major SPL metabolic and signaling genes in HCFs and HKCs with and without TGF-β treatment. Specifically, we tested the

TABLE 2. Cer composition of VitC-supplemented cultured HCFs and HKCs

	HCFs				HKCs			
Cer Species	Control	T1	T2	T3	Control	T1	T2	T3
C14:0	0.21 ± 0.02	0.22 ± 0.04	0.29 ± 0.06	0.31 ± 0.06	0.36 ± 0.05	0.29 ± 0.02[a]	0.35 ± 0.02	0.40 ± 0.04
C16:0	9.23 ± 0.80	6.14 ± 0.42[b]	8.43 ± 1.50	9.13 ± 1.32	11.22 ± 1.08[a]	8.75 ± 0.84[a,b]	8.89 ± 1.35	11.84 ± 1.60
C18:1	0.48 ± 0.42	0.02 ± 0.03	0.38 ± 0.33	0.32 ± 0.28	0.22 ± 0.39	0.00 ± 0.00	0.60 ± 0.57	0.42 ± 0.36
C18:0	1.33 ± 0.42	0.96 ± 0.27	1.66 ± 0.76	1.72 ± 0.19	3.13 ± 0.73	1.87 ± 0.54	3.09 ± 0.59	2.56 ± 0.07[a]
C20:0	0.45 ± 0.18	0.35 ± 0.09[b]	0.57 ± 0.16	0.58 ± 0.11	1.22 ± 0.35[a]	0.63 ± 0.17	1.12 ± 0.40	0.87 ± 0.15[a]
C22:0	1.72 ± 0.21	1.25 ± 0.15	1.91 ± 0.52	2.04 ± 0.39	3.02 ± 0.14[a]	2.07 ± 0.61	3.07 ± 0.74	2.77 ± 0.36
C24:1	4.77 ± 0.59	3.40 ± 0.36[b]	5.58 ± 0.57	5.53 ± 1.13	7.23 ± 1.31[a]	5.62 ± 0.48[a]	5.61 ± 1.11	7.99 ± 1.25
C24:0	3.17 ± 0.23	2.37 ± 0.44	3.80 ± 0.69	3.45 ± 0.32	5.55 ± 1.31[a]	4.27 ± 0.35[a]	4.81 ± 0.62	5.46 ± 0.58[a]
C26:1	0.27 ± 0.01	0.16 ± 0.02	0.21 ± 0.05	0.19 ± 0.03	0.23 ± 0.07	0.19 ± 0.01	0.19 ± 0.01	0.26 ± 0.05
C26:0	0.02 ± 0.01	0.01 ± 0.01	0.01 ± 0.01	0.01 ± 0.01	0.02 ± 0.01	0.02 ± 0.01	0.01 ± 0.01	0.02 ± 0.01
Total	21.63 ± 0.98	14.87 ± 1.59[b]	22.84 ± 4.44	23.27 ± 3.08	32.11 ± 1.23[a]	23.70 ± 2.02[a,b]	27.75 ± 3.10	32.59 ± 3.18[a]

Both cultures were treated with three isoforms of TGF-β, namely, T1, T2, and T3, as described in the Methods. Individual Cer species were quantitatively determined by UPLC-MS/MS and are presented as picomoles per milligram of cells (mean ± SD; n = 4).

[a] Statistically significant difference between HCFs and HKCs ($P \leq 0.01$).

[b] Indicates statistically significant difference between control and TGF-β-treated cells for both cell types.

expression of serine-palmitoyl transferase (*SPT*) *1*, *SPT2*, Cer synthase (*CerS*) *2*, *CerS4*, *SMPD1*, *ASAH1*, *SPHK1*, *SPHK2*, *S1P1*, and *S1P3* genes using real-time PCR. **Figure 5** shows the expression of these genes in HCFs and HKCs. *SMPD1* and *S1P3* were significantly upregulated in HKCs as compared with HCFs (Fig. 5; $P < 0.01$), where SPHK2 was significantly downregulated (Fig. 5; $P < 0.01$). No other genes showed significant regulation between the two cell types.

We further tested the effects of T1, T2, and T3 treatments on these genes in both cell types. In HCFs, we found that the T1 and T2 treatments significantly reduced the expression of the *CerS4* and *S1P3* genes (**Fig. 6A**; $P < 0.01$). The T3 treatment significantly reduced the expression of the *SPHK2* and *S1P3* genes, and both T1 and T2 treatments appeared to increase the expression of *S1P1* (Fig. 6A; $P < 0.01$).

In HKCs, we found an increase in the expression of *SPT2* with the T1 and T2 treatments and *CerS4* with the T2 treatment (Fig. 6B; $P < 0.01$). Both T1 and T3 treatments downregulated the expression of *SPHK1*; T1 treatment downregulated the expression of *S1P1*; and T3 treatment downregulated the expression of *S1P3* (Fig. 6B; $P < 0.01$).

Exogenous Cer/S1P stimulation leads to fibrotic phenotype in HCFs

Differences in Cer and S1P metabolism were found in HKCs, with HKCs showing greater levels than HCFs. Therefore, we asked whether these molecules were associated with the fibrotic phenotype of HKCs. To determine this, we treated both HCFs and HKCs with exogenous Cer (10 and 100 nM) and S1P (5 uM). The medium was changed every other day. After 2 weeks of treatment, we harvested the cells and assessed the major corneal fibrotic marker proteins, aSMA (ACT2), collagen-III, and TGF-β1.

S1P treatment, as well as treatment with both concentrations of Cer, increased aSMA expression 10- to 12-fold in HCFs (**Fig. 7A**; $P < 0.01$, n = 4). Although the baseline aSMA expression in HKCs was higher than HCFs, it was not significantly altered by either treatment (Fig. 7A). Compared with HCFs, Cer-treated HKCs had significantly higher levels of aSMA (Fig. 7A, $P < 0.05$, n = 4). Similar to aSMA, collagen-III levels in HKCs were higher than HCFs, whereas HKCs did not respond to either treatment (Fig. 7B). On the other hand, both S1P and Cer treatments significantly increased collagen-III levels by 5- to 8-fold in HCFs (Fig. 7B, $P < 0.05$); however, both S1P and Cer

TABLE 3. SM composition of VitC-supplemented cultured HCFs and HKCs

	HCF				HKC			
SM Species	Control	T1	T2	T3	Control	T1	T2	T3
C14:0	8.25 ± 1.78	5.60 ± 0.78	8.36 ± 2.19	7.11 ± 0.97	11.88 ± 3.16	14.44 ± 2.65	10.02 ± 4.03	15.52 ± 2.22[a]
C16:0	100.66 ± 7.96	69.15 ± 5.37	66.39 ± 9.44	67.94 ± 21.86	126.69 ± 33.81	95.42 ± 19.04	112.94 ± 15.03[a]	103.93 ± 13.38
C18:1	3.47 ± 2.54	1.32 ± 0.34	3.02 ± 0.81	2.50 ± 0.48	5.23 ± 1.48	6.31 ± 1.66	6.37 ± 2.14	6.15 ± 2.03
C18:0	35.63 ± 8.78	23.94 ± 6.64	42.94 ± 0.26	34.67 ± 12.48	46.19 ± 9.28	44.42 ± 5.28[a]	52.87 ± 15.94	42.98 ± 7.23
C20:0	7.59 ± 4.76	3.35 ± 0.91	9.23 ± 3.71	5.78 ± 0.83	14.99 ± 1.92	13.30 ± 2.30[a]	14.41 ± 3.741	13.18 ± 3.68[a]
C22:0	20.96 ± 5.99	11.80 ± 1.76	23.11 ± 4.64	17.57 ± 2.18	32.42 ± 1.18[a]	34.35 ± 3.06[a]	31.67 ± 4.81	32.34 ± 6.86[a]
C24:1	48.96 ± 3.44	32.81 ± 6.56[b]	53.75 ± 8.41	46.27 ± 5.23	63.03 ± 10.48	76.52 ± 9.02[a]	59.44 ± 16.75	81.39 ± 10.22[a]
C24:0	26.83 ± 2.03	18.68 ± 4.01[b]	30.32 ± 5.92	24.81 ± 2.94	37.13 ± 6.80	44.67 ± 5.27[a]	34.62 ± 6.82	44.44 ± 6.56[a]
C26:1	0.67 ± 0.04	0.56 ± 0.15	0.90 ± 0.19	0.75 ± 0.15	0.93 ± 0.21	1.17 ± 0.20[a]	0.90 ± 0.34	1.45 ± 0.24[a]
C26:0	0.44 ± 0.09	0.25 ± 0.04	0.35 ± 0.05	0.87 ± 0.12[a]	0.61 ± 0.11	0.73 ± 0.18	0.50 ± 0.41	0.90 ± 0.14[a]
Total	253.49 ± 30.54	167.54 ± 10.87[b]	238.62 ± 33.12	207.91 ± 25.49	339.17 ± 30.9	331.42 ± 29.97	323.96 ± 31.75[a]	342.17 ± 46.61[a]

Both cultures were treated with three isoforms of TGF-β, namely, T1, T2, and T3, as described in the Methods. Individual SM species were quantitatively determined by UPLC-MS/MS and are presented as picomoles per milligram of cells (mean ± SD; n = 4).

[a] Statistically significant difference between HCFs and HKCs ($P \leq 0.01$).

[b] Indicates statistically significant difference between control and TGF-β-treated cells for both the cell types.

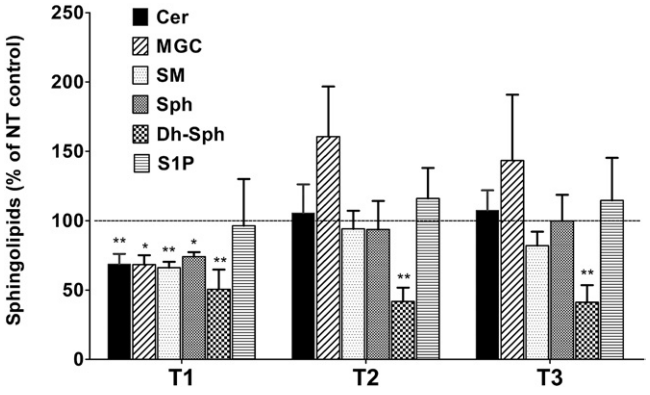

Fig. 3. Alteration in SPL composition of cultured HCFs treated with three isoforms of TGF-β (T1, T2, and T3). The total absolute quantity (picomoles per milligram of cells) of the major SPL species from HCFs treated with T1, T2, and T3 were analyzed with LC-MS/MS and are presented here with respect to the untreated controls. $*P \leq 0.01$ (n = 4) and $**P \leq 0.001$ (n = 4) indicate the statistically significant difference from the untreated controls. NT, no treatment.

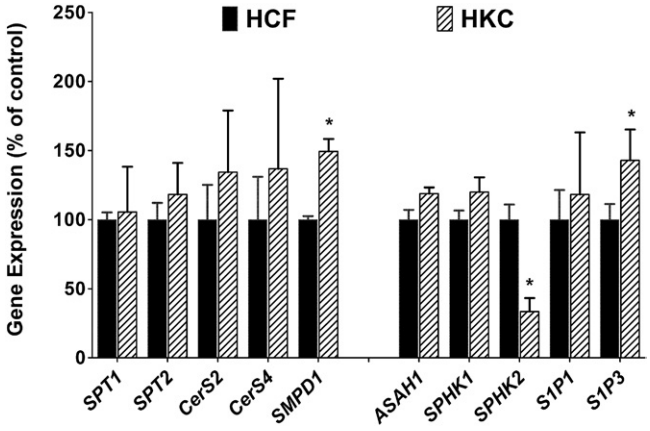

Fig. 5. Expression of SPL metabolic genes in cultured HCFs and HKCs. Expression of some major SPL metabolic and signaling genes were determined by qRT-PCR. Expression values are presented relative to the control (HCFs = 100) ($*P \leq 0.01$, n = 4).

treatments did not modulate TGF-β1 in HCFs and HKCs. In our model, exogenous S1P and Cer led to significant increases of corneal fibrotic markers on HCFs, providing strong support for the role of bioactive SPLs (Cer and S1P) in the fibrotic development in corneal cells. The endogenous increase of these lipids in HKCs supports this hypothesis and suggests an intimate mechanistic link between these SPLs, the human corneal stromal cells, and the development of KC.

Inhibition of Cer and rescuing of HKC phenotype

To provide further evidence for this hypothesis, we inhibited Cer synthesis in HKCs and tested to determine whether we could reverse the fibrotic nature of these cells. We used a known Cer synthesis inhibitor, FTY720, in order to determine whether the HKC phenotype could be reversed or rescued by reducing the Cer generation. We treated both HCFs and HKCs with varied doses of FTY720, starting with 10 nM followed by 1 and 10 uM. After 2 weeks of treatment (changing the medium every other day), we harvested the cells and analyzed for SPL composition and the expression of the major corneal fibrotic marker genes.

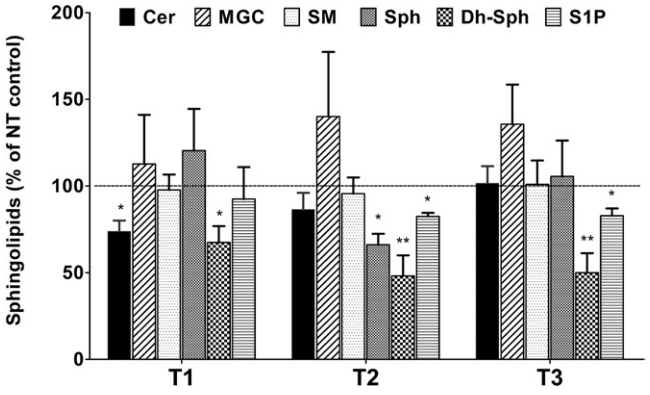

Fig. 4. Alteration in SPL composition of cultured HKCs treated with three isoforms of TGF-β (T1, T2, and T3). The total absolute quantity (picomoles per milligram of cells) of the major SPL species from HKCs treated with T1, T2, and T3 were analyzed with LC-MS/MS and are presented here with respect to the untreated controls. $*P \leq 0.01$ (n = 4) and $**P \leq 0.001$ (n = 4) indicate the statistically significant difference from the untreated controls. NT, no treatment.

We found that all three doses of FTY720 reduced the total Cer in HKCs significantly (**Fig. 8A**; $P < 0.001$, n = 4). However, the same treatment did not affect the levels of MGC and SM (data not shown). Very interestingly, HCFs were found to be resistant to FTY720 treatment, as we did not see any change in Cer levels in these cells (data not shown). As there are at least six CerSs that have some preference for Cer fatty acid chain length, we wanted to see whether the effect was specific to a particular species of Cer or whether all species were affected similarly in HKC cells. We found that the two most abundant Cer species (C24:0 and C24:1), which are longer chain Cers, were reduced significantly with all doses of FTY720 (Fig. 8B; $P < 0.001$, n = 4). We also investigated the minor signaling SPLs and found that Sph and S1P levels were decreased with the lowest dose of FTY720, but not with the higher doses, in HKCs (Fig. 8C; $P < 0.01$, n = 4). However, only Dh-Sph was found to be decreased with a higher dose of FTY720 (Fig. 8C; $P < 0.01$, n = 4).

We then investigated the regulation of three major fibrotic marker genes in the human cornea: TGF-β1, aSMA (ACT2), and collagen-III. **Figure 9** shows regulation of these three genes in HCFs (Fig. 9A) and HKCs (Fig. 9B). HCFs showed no significant regulation of any of these three genes with any of the FTY720 concentrations tested here (Fig. 9A). As is very evident from the expression data, HKCs have significantly higher levels of TGF-β1 cells (>2-fold), ACT2 cells (>4-fold), and collagen-III cells (>15-fold) when compared with HCFs (Fig. 9B; $P < 0.001$, n = 4). FTY720 treatment had the biggest impact at 10 uM, where TGF-β1 levels between HCFs and HKCs were identical (Fig. 9B; $P < 0.01$, n = 4). aSMA showed a downregulation with increasing FTY720 concentration, with significance shown at 10 uM of FTY720 (Fig. 9B; $P < 0.001$, n = 4). Collagen-III expression showed an identical trend to aSMA between HCFs and HKCs (Fig. 9A, B). Collagen-III was significantly

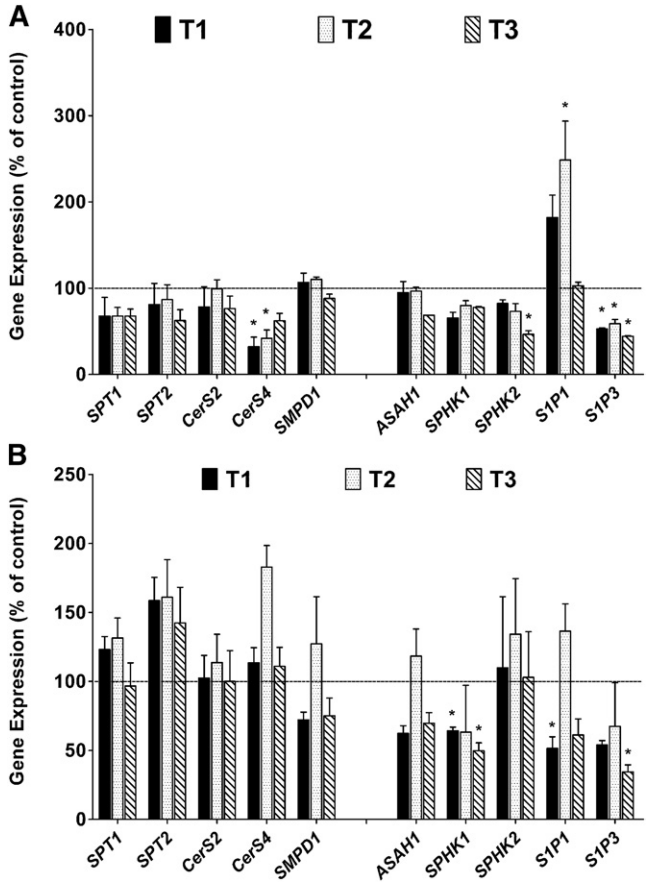

Fig. 6. Alteration in SPL metabolic genes in HCFs (A) and in HKCs (B) treated with three isoforms of TGF-β (T1, T2, and T3). Expression of the genes presented in Fig. 5 was compared between untreated and treated HCFs (A) and HKCs (B) with either T1, T2, or T3. Expression values are presented relative to the untreated controls (controls = 100) (*$P \leq 0.01$, n = 4).

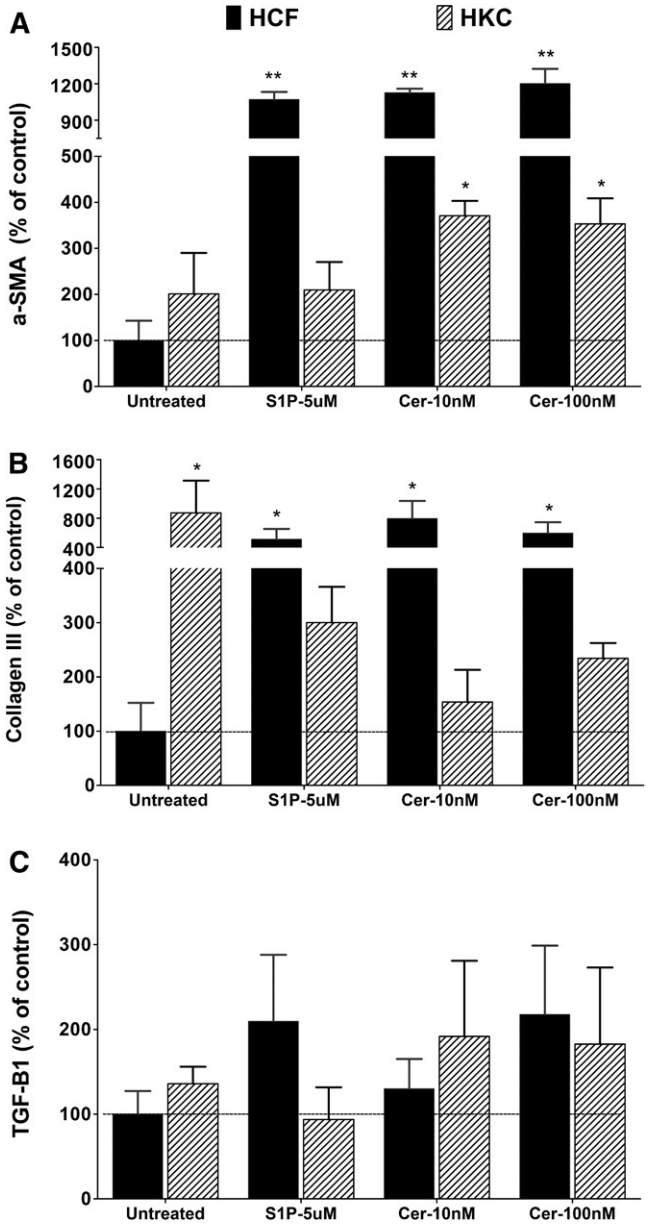

Fig. 7. Expression of fibrosis marker proteins in cultured HCFs and HKCs treated with S1P and Cer. Expression of aSMA (ACTA2) (A), collagen-III (B), and TGF-β1 (TGF-B1) (C) were determined by Western blotting and the levels were determined by densitometric analysis using GAPDH as control. Expression values are presented relative to the untreated control (HCFs = 100). * $P < 0.01$ (n = 4) and ** $P < 0.001$ (n = 4) indicate the statistically significant difference from the untreated HCF.

downregulated in HKCs, in a dose-dependent manner, following stimulation with FTY720. In our model, FTY720 mediated significant decreases of corneal fibrotic markers, suggesting a reversal of the myofibroblastic HKC phenotype at gene expression level. These results support our previous findings that HKCs are more myofibroblastic than the healthy HCFs and indicate a potential role for Cer inhibition in reducing the fibrosis in KC.

DISCUSSION

KC is the most common cause of corneal transplants worldwide. Despite much scientific advancement, we still do not fully understand the pathophysiology of the disease. Most genetic studies are inconclusive and there is no animal model to study the disease (47). In 2012, our group introduced the first 3D in vitro model that could mimic the disease in vivo (19). Since then, we have reported several inherent problems found in cells isolated from KC patients (31, 48). Among others, we have shown metabolic dysfunctions and overexpression of fibrotic markers. The current study aimed to advance our knowledge about HKCs and their SPL profile.

To our knowledge, no study has been done on SPL composition and signaling in HCFs or on HKCs. We generated novel data and provided information on the potential role of SPL signaling in healthy and KC corneal cells. We found by culturing in similar conditions that HKCs contain higher levels of Cer and S1P (Fig. 2). Cer and S1P are the major cellular SPLs involved in signaling (21, 23). Although Cer is the key molecule of cellular SPL synthesis and one of the key products of degradation in lysosomes, its level is very tightly regulated by several anabolic and catabolic enzymes.

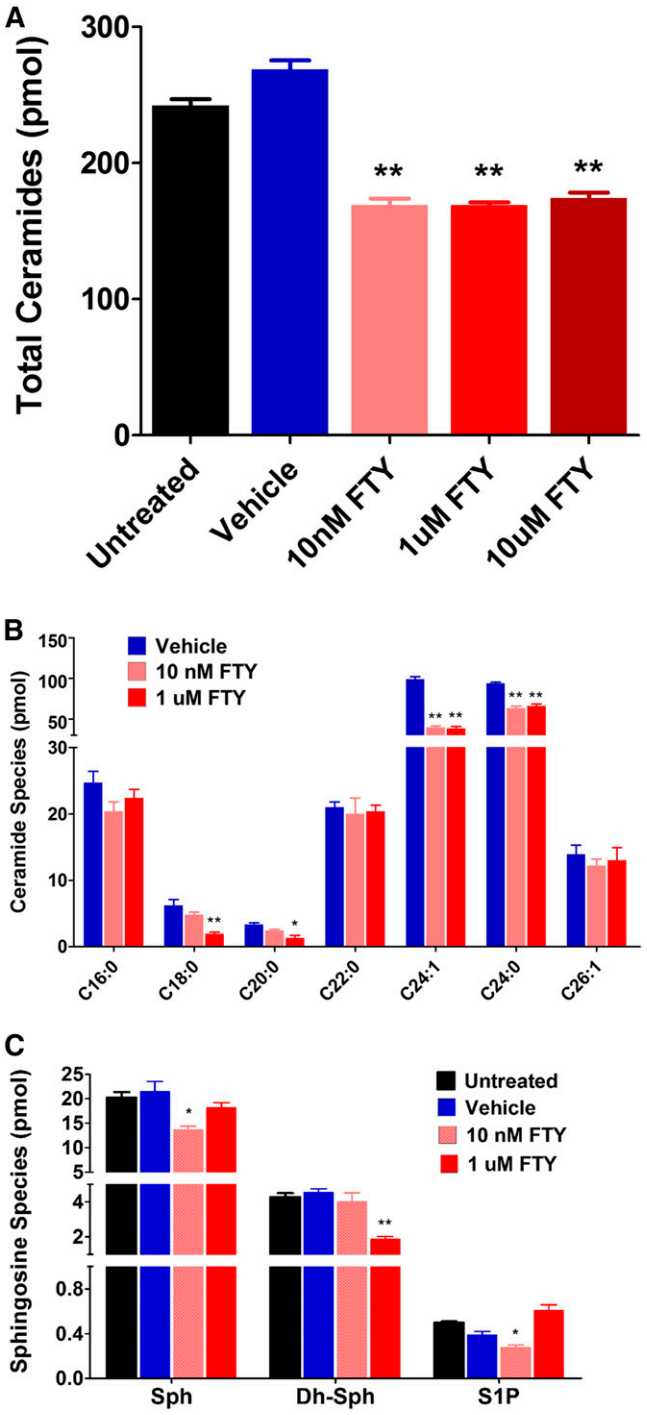

Fig. 8. SPL composition changes in cultured HKCs after treatment with FTY720. A: The absolute quantity (picomoles per milligram of cells) of total Cers was analyzed with LC-MS/MS and measured after treatment with FTY720 (FTY) or vehicle. The level of total Cers was significantly (**$P < 0.001$) reduced after the treatment and there was no dose effect. B: The major species of individual Cers measured after FTY720 treatment. Vehicle-treated cells were not different from the controls (not shown here) and, therefore, were not included here. Long-chain Cers are significantly reduced after FTY720 treatment (*$P < 0.01$; **$P < 0.001$). C: S1P metabolites in HKCs with FTY720 treatment. Minor signaling SPLs, Sph, Dh-Sph, and S1P, were also analyzed with LC-MS/MS. Low-dose FTY720 (10 nM) appears to affect the levels of Sph and S1P, but not the higher dose (1 uM). The higher dose reduced the levels of Dh-Sph significantly (*$P < 0.01$; **$P < 0.001$).

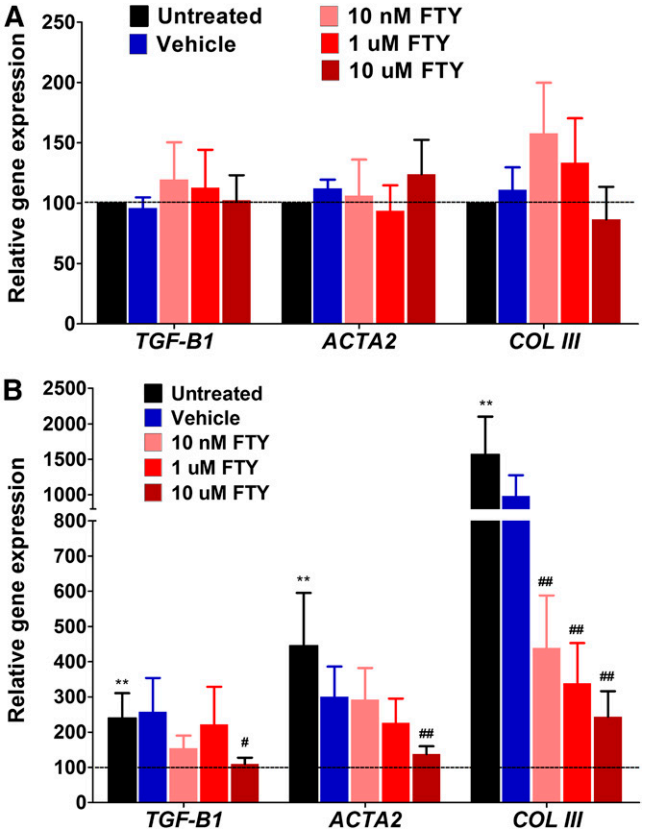

Fig. 9. Expression of fibrosis marker genes in cultured normal HCFs and HKCs treated with FTY720. Expression of TGF-β1 (TGF-B1), aSMA (ACTA2), and collagen-III (COL III) were determined by qRT-PCR using TaqMan probes. Expression values are presented relative to the untreated control (HCFs = 100). A: HCFs treated with FTY720 (FTY); none of the genes showed any variation in expression. B: HKCs treated with FTY720. Untreated cells have very significantly higher expression of these fibrotic marker genes compared with HCFs (black bars; **$P < 0.001$, n = 4). All doses of FTY720 reduced COL III expression significantly (##$P < 0.001$); whereas, the high dose (10 uM FTY20) reduced the expression of TGB-β1 and ACTA2 (#$P < 0.01$; ##$P < 0.001$).

An increase in level is commonly associated with inducing inflammatory and apoptotic pathways (49–51). In the cell membrane, free Cer generated from SM can have pleotropic effects: altering receptor functioning, inducing death signals, inhibiting the cell survival pathway by blocking Akt, or changing the mitochondrial transmembrane potential and thereby releasing cytochrome c and activating Casp1 (52). Increased Cers also serve as the source of S1P. S1P signaling is very much associated with various types of cellular signaling that include cell adhesion, migration, proliferation, etc. (21, 25, 53). The increase of Cer and S1P in KC cells is very interesting and could be related to increased synthesis of de novo Cer or breakdown of higher order SPLs, such as SM. However, here we found that the level of SM appeared to be high in HKCs, but not significantly high (Fig. 2). The cellular abundance of SM is much higher than Cer in every cell. Here, we found that SM abundance was >10-fold that of Cer in human corneal cells. Therefore, it is possible that a small percentage of changes in SM may contribute to the ~50% increase in Cer

(Fig. 2). When we checked gene expression, we found no changes in de novo biosynthetic genes, but an increase in expression of acid sphingomyelinase (SMPD1) (Fig. 5), which suggests that the increased Cer in HKCs might have resulted from breakdown of SM. However, we do not know whether there was any alteration in the activity of the enzymes. The increase in S1P could have resulted from higher levels of Cer, although we did not see any changes in the expression of the genes responsible for S1P generation, such as acid ceramidase (ASAH1) and SPHK1. Instead, we saw a decrease in SPHK2 (Fig. 5), which, however, does not reflect their protein levels or enzyme activity. The increase of Cer and S1P in HKCs could be one of the causes of the development of the HKC phenotype by inducing the pathways that promote the expression of fibrotic markers and the increased secretion of collagen, or these could be consequences of the intrinsic changes in the HKCs for genetic reasons.

In order to determine whether Cer and S1P are key metabolic factors for fibrotic development in corneal cells, we investigated whether stimulation of normal corneal fibroblasts with exogenous Cer and S1P would induce fibrogenesis in our 3D model system. We found that both stimuli (Cer and S1P) induced significant upregulation of fibrotic proteins (aSMA and collagen-III) in HCFs (Fig. 7). However, HKCs, which are already fibrotic and contain higher levels of endogenous Cer and S1P, do not respond to excess exogenous lipids (Fig. 7). Therefore, using an alternative approach for HKC cells, Cer generation was inhibited in the HKCs via FTY720, which is a known potent inhibitor of Cer synthesis via the de novo pathway. As expected, we found a significant reduction of total Cer in HKCs in a dose-independent manner (Fig. 8). Interestingly, this reduction in Cer was associated with a reduction in the three major fibrotic markers tested (Fig. 9). Activation of SPHK and the role of S1P have been demonstrated to be involved in the process of fibrogenesis in various cell types (54–56). However, to our knowledge, a direct effect of Cer on the expression of fibrotic genes and proteins has not been described. It is quite possible that a portion of the increased endogenous Cer in HKCs, or exogenously added Cer in culture, is metabolized and produces S1P, thereby generating the fibrogenesis effect observed (Fig. 7). Therefore, we propose that: *1*) dysregulation of SPL metabolism is associated with fibrotic development in corneal cells; *2*) Cer and S1P can induce overexpression of myofibroblastic proteins, such as aSMA and collagen-III, and transform nonfibrotic corneal cells to become fibrotic; and *3*) the fibrotic nature of HKCs, as seen in human KC, can be reversed by inhibiting endogenous Cer and, thus, S1P (Cer is the precursor for S1P).

FTY720 is a known inhibitor of CerS and blocks de novo Cer production (57–59). In previous publications, we demonstrated the inhibitory effect of FTY720 in in vivo retinas (36, 44). Cellular Cers are synthesized by CerSs, one of the six different CerSs (CerS1–6) found in mammalian system. The chain length of Cer depends on the activity of the specific CerSs. CerS1 synthesizes mainly C18-Cer; CerS4 synthesizes C18-/C20-/C24-Cer; CerS5 and CerS6 synthesize mostly C14-/C16-/C18-Cer; CerS2 synthesizes preferentially C22-/C24-Cer; and CerS3 synthesizes very long-chain Cers (>C26-Cer) (60–63). FTY720 can inhibit all of the six CerS isozymes, with CerS4 being the least inhibited (57–59). In vitro kinetic studies suggest that FTY720 is a potent and competitive inhibitor of CerS2, compared with the classical CerS inhibitor, fumonisin B1, that inhibits the de novo biosynthesis of 24:1 and 24:0-Cers (57). We found that the species of Cer that are majorly inhibited by FTY720 are 24:1 and 24:0-Cers (Fig. 8), which verily supports the FTY720 inhibitory action on CerS2. Thus, our studies establish for the first time that: *1*) dysregulation of Cer synthesis is associated with the KC phenotype (at least at cellular levels); *2*) out of the six CerSs, CerS2 appears to play the major role in the production of higher levels of longer chain Cers and this can be targeted for therapeutic development; and *3*) CerS inhibitors, like FTY720, have the potential to be developed as therapeutic agents for human KC.

While studying SPL-TGF relationships in HCFs, we found that T1 treatment reduced the levels of all species of SPLs, except S1P; whereas, T2 and T3 treatments reduced only the level of Dh-Sph (Fig. 3). Reduction in Dh-Sph indicates a blockage in the very first step of de novo Cer synthesis; gene expression analysis of SPT1 and SPT2, the enzymes responsible for this step, showed a trend of reduction in SPT1 by all the TGF-β isoforms (Fig. 6). However, this reduction could have resulted from many other factors, such as availability of substrates, inhibition of enzyme activity, etc. Both T1 and T2 treatments suppressed the expression of the CerS4 gene; the CERS4 enzyme is responsible for synthesizing Cers with C18, C20, and C24 fatty acid chains (64, 65). This might have contributed to the lower levels of Cer in T1-treated HCFs and HKCs (Fig. 3, Table 2).

In HKCs, T1 treatment reduced the levels of Cer and Dh-Sph; T2 treatment reduced the levels of Sph, Dh-Sph, and S1P; and T3 treatment reduced the levels of Dh-Sph and S1P (Fig. 4). In this study (Figs. 7, 9) and in previous studies, we have shown that HKCs express higher levels of fibrotic markers, such as SMA and collagen-III, when compared with HCFs, and that TGF-β3 is effective in downregulating these fibrotic markers (18, 30, 33, 34). T3-mediated downregulation of S1P in HKCs might suggest that S1P plays a role in the fibrotic phenotype in HKCs and T3 suppresses this mediator either at the gene expression level or at the enzyme activity level. It is also clear from our data that all forms of TGF can suppress de novo biosynthesis of SPLs, as evident from the reduction of the very first product of this pathway, Dh-Sph (Figs. 3, 4). Thus, TGFs and FTY720 appear to act on a similar axis by reducing de novo Cer biosynthesis. Dysregulation of de novo Cer biosynthesis could therefore be a key factor for developing KC.

From the gene expression analysis, it is evident that the T1 and T3 treatments had almost similar effects on HKCs, especially with regard to S1P generation and signaling genes. Both factors reduced the expression of SMPD1, ASAH1, SPHK1, and S1P3 in HKCs (Fig. 6). The S1P3 receptor appears to be dysregulated (overexpressed) in HKCs. All the isoforms of TGF-β reduced the expression of S1P3 in HCFs, but only T3 appeared to be effective in

reducing the levels of S1P3 expression in HKCs (Fig. 6). S1P3 is a G protein-coupled receptor that can be involved in a multitude of cellular signaling pathways because it can activate G12/13, Gq, or Gi. G12/13 activates Rho kinase, whereas Gq and Gi activate PLC, Ras/Raf pathways. Ras/Raf activates ERK and followed by AP-1 transcription factor to increase expression of CTGF and ECM genes. (66). S1P3 is also known to work through the Smad pathway (Smad 1, 2, 3, and 4) in association with the TGF receptor pathway to increase ECM proteins (67). Increase in S1P3 expression in HKCs may therefore be related to its higher levels of ECM production. TGB isoforms induced reduction of S1P3 expression in HCF and by T3 in HKCs may therefore be related to the reduction in ECM production in these cells upon TGF-β treatments.

Our current study is focused on SPL metabolism and signaling in HKCs and we have correlated our findings with mRNA levels. This is mainly due to the complex nature of SPL metabolism and not having enough tools and resources to investigate each and every enzyme in the pathway at protein and activity levels. We assumed that mRNA concentration would correlate well with mRNA protein concentrations in a steady-state cellular environment. We are aware of the fact that mRNA and protein concentration depends on multiple factors. mRNA levels are affected by transcriptional regulation, post-transcriptional regulation that affects RNA stability. Protein levels, on the other hand, are affected by translational regulation, protein stability, and modification and therefore the levels of mRNA and protein for a gene do not always correlate well. (68). In general, the cellular concentrations of proteins correlate with the abundances of their corresponding mRNAs at ~40% correlation (69, 70). However, in a homogeneous cell population or in single cells, this correlation may go as high as 63% (71). Future studies will dissect a small set of key genes and investigate their role further, including at the protein level. Such studies could produce confirmatory evidence to the mRNA-lipid correlation found in this study.

In conclusion, we found increases in the signaling SPLs (Cer and S1P) in HKCs not found in HCFs grown in similar conditions in vitro. We determined that stimulation of normal human corneal cells with Cer and S1P can transform them into myofibroblastic cells. Additionally, we showed that treatment with the CerS inhibitor, FTY720, could reverse the fibrotic phenotype of the HKCs. Treatment with TGF-β1 reversed the increase in Cer in HKCs and treatment with TGF-β3 reversed the increase in S1P. This indicates that fibrotic development in HKCs has SPL involvement and that the TGF-β pathway intersects with the SPL pathway. The fine relationship of these two pathways needs further investigation. Gene expression studies suggested that an increase in *S1P3* receptor mRNA in HKCs could be reduced to normal levels upon TGF-β3 treatment. We previously demonstrated that TGF-β3 can reverse the fibrotic phenotype of HKCs; this study suggests a possible mechanism of TGF-β3 action, which could suppress S1P metabolism as well as S1P signaling through the S1P3 receptor. Furthermore, this study demonstrates an association of SPL signaling in fibrotic corneal development, such as in cases of human KC.

The authors acknowledge the editorial help provided by Dr. Lynda Wilmott from University of Tennessee Health Sciences Center, Memphis, TN.

REFERENCES

1. Kennedy, R. H., W. M. Bourne, and J. A. Dyer. 1986. A 48-year clinical and epidemiologic study of keratoconus. *Am. J. Ophthalmol.* **101:** 267–273.
2. McMahon, T. T., T. B. Edrington, L. Szczotka-Flynn, H. E. Olafsson, L. J. Davis, K. B. Schechtman, and C. S. Group. 2006. Longitudinal changes in corneal curvature in keratoconus. *Cornea.* **25:** 296–305.
3. Rabinowitz, Y. S. 1998. Keratoconus. *Surv. Ophthalmol.* **42:** 297–319.
4. Romero-Jiménez, M., J. Santodomingo-Rubido, and J. S. Wolffsohn. 2010. Keratoconus: a review. *Cont. Lens Anterior Eye.* **33:** 157–166, quiz 205.
5. Zadnik, K., J. T. Barr, M. O. Gordon, and T. B. Edrington. 1996. Biomicroscopic signs and disease severity in keratoconus. *Cornea.* **15:** 139–146.
6. Brierly, S. C., L. Izquierdo, Jr., and M. J. Mannis. 2000. Penetrating keratoplasty for keratoconus. *Cornea.* **19:** 329–332.
7. Sray, W. A., E. J. Cohen, C. J. Rapuano, and P. R. Laibson. 2002. Factors associated with the need for penetrating keratoplasty in keratoconus. *Cornea.* **21:** 784–786.
8. Ihalainen, A. 1986. Clinical and epidemiological features of keratoconus genetic and external factors in the pathogenesis of the disease. *Acta Ophthalmol. Suppl.* **178:** 1–64.
9. Priyadarsini, S., J. Hjortdal, A. Sarker-Nag, H. Sejersen, J. M. Asara, and D. Karamichos. 2014. Gross cystic disease fluid protein-15/prolactin-inducible protein as a biomarker for keratoconus disease. *PLoS One.* **9:** e113310.
10. Karamichos, D., J. D. Zieske, H. Sejersen, A. Sarker-Nag, J. M. Asara, and J. Hjortdal. 2015. Tear metabolite changes in keratoconus. *Exp. Eye Res.* **132:** 1–8.
11. Gupta, A., D. Monroy, Z. Ji, K. Yoshino, A. Huang, and S. C. Pflugfelder. 1996. Transforming growth factor beta-1 and beta-2 in human tear fluid. *Curr. Eye Res.* **15:** 605–614.
12. Burdon, K. P., S. Macgregor, Y. Bykhovskaya, S. Javadiyan, X. Li, K. J. Laurie, D. Muszynska, R. Lindsay, J. Lechner, and T. Haritunians. 2011. Association of polymorphisms in the hepatocyte growth factor gene promoter with keratoconus. *Invest. Ophthalmol. Vis. Sci.* **52:** 8514–8519.
13. Toprak, I., V. Kucukatay, C. Yildirim, E. Kilic-Toprak, and O. Kilic-Erkek. 2014. Increased systemic oxidative stress in patients with keratoconus. *Eye (Lond.).* **28:** 285–289.
14. Berk, A. T., A. O. Saatci, M. D. Erçal, M. Tunç, and M. Ergin. 1996. Ocular findings in 55 patients with Down's syndrome. *Ophthalmic Genet.* **17:** 15–19.
15. Guo, X., A. E. Hutcheon, S. A. Melotti, J. D. Zieske, V. Trinkaus-Randall, and J. W. Ruberti. 2007. Morphologic characterization of organized extracellular matrix deposition by ascorbic acid-stimulated human corneal fibroblasts. *Invest. Ophthalmol. Vis. Sci.* **48:** 4050–4060.
16. Karamichos, D., X. Q. Guo, A. E. Hutcheon, and J. D. Zieske. 2010. Human corneal fibrosis: an in vitro model. *Invest. Ophthalmol. Vis. Sci.* **51:** 1382–1388.
17. Karamichos, D., A. E. Hutcheon, C. B. Rich, V. Trinkaus-Randall, J. M. Asara, and J. D. Zieske. 2014. In vitro model suggests oxidative stress involved in keratoconus disease. *Sci. Rep.* **4:** 4608.
18. Karamichos, D., A. E. Hutcheon, and J. D. Zieske. 2014. Reversal of fibrosis by TGF-beta3 in a 3D in vitro model. *Exp. Eye Res.* **124:** 31–36.
19. Karamichos, D., R. Zareian, X. Guo, A. Hutcheon, J. Ruberti, and J. Zieske. 2012. Novel in vitro model for keratoconus disease. *J. Funct. Biomater.* **3:** 760–775.
20. Shimizu, T. 2009. Lipid mediators in health and disease: enzymes and receptors as therapeutic targets for the regulation of immunity and inflammation. *Annu. Rev. Pharmacol. Toxicol.* **49:** 123–150.

21. Chalfant, C. E., and S. Spiegel. 2005. Sphingosine 1-phosphate and ceramide 1-phosphate: expanding roles in cell signaling. *J. Cell Sci.* **118:** 4605–4612.
22. Gangoiti, P., L. Camacho, L. Arana, A. Ouro, M. H. Granado, L. Brizuela, J. Casas, G. Fabrias, J. L. Abad, A. Delgado, et al. 2010. Control of metabolism and signaling of simple bioactive sphingolipids: Implications in disease. *Prog. Lipid Res.* **49:** 316–334.
23. Hannun, Y. A., and L. M. Obeid. 2008. Principles of bioactive lipid signalling: lessons from sphingolipids. *Nat. Rev. Mol. Cell Biol.* **9:** 139–150.
24. Maceyka, M., and S. Spiegel. 2014. Sphingolipid metabolites in inflammatory disease. *Nature.* **510:** 58–67.
25. Hla, T. 2003. Signaling and biological actions of sphingosine 1-phosphate. *Pharmacol. Res.* **47:** 401–407.
26. Ikeda, H., N. Watanabe, I. Ishii, T. Shimosawa, Y. Kume, T. Tomiya, Y. Inoue, T. Nishikawa, N. Ohtomo, Y. Tanoue, et al. 2009. Sphingosine 1-phosphate regulates regeneration and fibrosis after liver injury via sphingosine 1-phosphate receptor 2. *J. Lipid Res.* **50:** 556–564.
27. Li, C., X. Jiang, L. Yang, X. Liu, S. Yue, and L. Li. 2009. Involvement of sphingosine 1-phosphate (SIP)/S1P3 signaling in cholestasis-induced liver fibrosis. *Am. J. Pathol.* **175:** 1464–1472.
28. Li, C., S. Zheng, H. You, X. Liu, M. Lin, L. Yang, and L. Li. 2011. Sphingosine 1-phosphate (S1P)/S1P receptors are involved in human liver fibrosis by action on hepatic myofibroblasts motility. *J. Hepatol.* **54:** 1205–1213.
29. Pyne, N. J., G. Dubois, and S. Pyne. 2013. Role of sphingosine 1-phosphate and lysophosphatidic acid in fibrosis. *Biochim. Biophys. Acta.* **1831:** 228–238.
30. Priyadarsini, S., T. B. McKay, A. Sarker-Nag, and D. Karamichos. 2015. Keratoconus in vitro and the key players of the TGF-beta pathway. *Mol. Vis.* **21:** 577–588.
31. Lyon, D., T. B. McKay, A. Sarkar-Nag, S. Priyadarsini, and D. Karamichos. 2015. Human keratoconus cell contractility is mediated by transforming growth factor-beta isoforms. *J. Funct. Biomater.* **6:** 422–438.
32. Priyadarsini, S., A. Sarker-Nag, J. Allegood, C. Chalfant, and D. Karamichos. 2015. Description of the sphingolipid content and subspecies in the diabetic cornea. *Curr. Eye Res.* **40:** 1204–1210.
33. Karamichos, D., C. B. Rich, R. Zareian, A. E. Hutcheon, J. W. Ruberti, V. Trinkaus-Randall, and J. D. Zieske. 2013. TGF-beta3 stimulates stromal matrix assembly by human corneal keratocyte-like cells. *Invest. Ophthalmol. Vis. Sci.* **54:** 6612–6619.
34. Karamichos, D., A. E. Hutcheon, and J. D. Zieske. 2011. Transforming growth factor-beta3 regulates assembly of a non-fibrotic matrix in a 3D corneal model. *J. Tissue Eng. Regen. Med.* **5:** e228–e238.
35. Chen, H., J. T. Tran, R. E. Anderson, and M. N. Mandal. 2012. Caffeic acid phenethyl ester protects 661W cells from H2O2-mediated cell death and enhances electroretinography response in dim-reared albino rats. *Mol. Vis.* **18:** 1325–1338.
36. Chen, H., J. T. Tran, A. Eckerd, T. P. Huynh, M. H. Elliott, R. S. Brush, and N. A. Mandal. 2013. Inhibition of de novo ceramide biosynthesis by FTY720 protects rat retina from light-induced degeneration. *J. Lipid Res.* **54:** 1616–1629.
37. Mandal, M. N., and R. Ayyagari. 2006. Complement factor H: spatial and temporal expression and localization in the eye. *Invest. Ophthalmol. Vis. Sci.* **47:** 4091–4097.
38. Mandal, M. N., G. P. Moiseyev, M. H. Elliott, A. Kasus-Jacobi, X. Li, H. Chen, L. Zheng, O. Nikolaeva, R. A. Floyd, J. X. Ma, et al. 2011. Alpha-phenyl-N-tert-butylnitrone (PBN) prevents light-induced degeneration of the retina by inhibiting RPE65 protein isomerohydrolase activity. *J. Biol. Chem.* **286:** 32491–32501.
39. Mandal, M. N., V. Vasireddy, M. M. Jablonski, X. Wang, J. R. Heckenlively, B. A. Hughes, G. B. Reddy, and R. Ayyagari. 2006. Spatial and temporal expression of MFRP and its interaction with CTRP5. *Invest. Ophthalmol. Vis. Sci.* **47:** 5514–5521.
40. Schmittgen, T. D., and K. J. Livak. 2008. Analyzing real-time PCR data by the comparative CT method. *Nat. Protoc.* **3:** 1101–1108.
41. McKay, T. B., A. Sarker-Nag, D. Lyon, J. M. Asara, and D. Karamichos. 2015. Quercetin modulates keratoconus metabolism in vitro. *Cell Biochem. Funct.* **33:** 341–350.
42. McKay, T. B., D. Lyon, A. Sarker-Nag, S. Priyadarsini, J. M. Asara, and D. Karamichos. 2015. Quercetin attenuates lactate production and extracellular matrix secretion in keratoconus. *Sci. Rep.* **5:** 9003.
43. Simanshu, D. K., R. K. Kamlekar, D. S. Wijesinghe, X. Zou, X. Zhai, S. K. Mishra, J. G. Molotkovsky, L. Malinina, E. H. Hinchcliffe, C. E. Chalfant, et al. 2013. Non-vesicular trafficking by a ceramide-1-phosphate transfer protein regulates eicosanoids. *Nature.* **500:** 463–467.
44. Stiles, M., H. Qi, E. Sun, J. Tan, H. Porter, J. Allegood, C. E. Chalfant, D. Yasumura, M. T. Matthes, M. M. LaVail, et al. 2016. Sphingolipid profile alters in retinal dystrophic P23H-1 rats and systemic FTY720 can delay retinal degeneration. *J. Lipid Res.* **57:** 818–831.
45. Wijesinghe, D. S., J. C. Allegood, L. B. Gentile, T. E. Fox, M. Kester, and C. E. Chalfant. 2010. Use of high performance liquid chromatography-electrospray ionization-tandem mass spectrometry for the analysis of ceramide-1-phosphate levels. *J. Lipid Res.* **51:** 641–651.
46. Wijesinghe, D. S., M. Brentnall, J. A. Mietla, L. A. Hoeferlin, R. F. Diegelmann, L. H. Boise, and C. E. Chalfant. 2014. Ceramide kinase is required for a normal eicosanoid response and the subsequent orderly migration of fibroblasts. *J. Lipid Res.* **55:** 1298–1309.
47. Rabinowitz, Y. S. 2003. The genetics of keratoconus. *Ophthalmol. Clin. North Am.* **16:** 607–620.
48. Sarker-Nag, A., A. E. Hutcheon, and D. Karamichos. 2016. Mitochondrial profile and responses to TGF-β ligands in keratoconus. *Curr. Eye Res.* **41:** 900–907.
49. Chen, H., J. T. Tran, R. S. Brush, A. Saadi, A. K. Rahman, M. Yu, D. Yasumura, M. T. Matthes, K. Ahern, H. Yang, et al. 2012. Ceramide signaling in retinal degeneration. *Adv. Exp. Med. Biol.* **723:** 553–558.
50. Hannun, Y. A. 1996. Functions of ceramide in coordinating cellular responses to stress. *Science.* **274:** 1855–1859.
51. Obeid, L. M., C. M. Linardic, L. A. Karolak, and Y. A. Hannun. 1993. Programmed cell death induced by ceramide. *Science.* **259:** 1769–1771.
52. Nixon, G. F. 2009. Sphingolipids in inflammation: pathological implications and potential therapeutic targets. *Br. J. Pharmacol.* **158:** 982–993.
53. Watterson, K., H. Sankala, S. Milstien, and S. Spiegel. 2003. Pleiotropic actions of sphingosine-1-phosphate. *Prog. Lipid Res.* **42:** 344–357.
54. Sobel, K., K. Menyhart, N. Killer, B. Renault, Y. Bauer, R. Studer, B. Steiner, M. H. Bolli, O. Nayler, and J. Gatfield. 2013. Sphingosine 1-phosphate (S1P) receptor agonists mediate pro-fibrotic responses in normal human lung fibroblasts via S1P2 and S1P3 receptors and Smad-independent signaling. *J. Biol. Chem.* **288:** 14839–14851.
55. Shiohira, S., T. Yoshida, H. Sugiura, M. Nishida, K. Nitta, and K. Tsuchiya. 2013. Sphingosine-1-phosphate acts as a key molecule in the direct mediation of renal fibrosis. *Physiol. Rep.* **1:** e00172.
56. Swaney, J. S., K. M. Moreno, A. M. Gentile, R. A. Sabbadini, and G. L. Stoller. 2008. Sphingosine-1-phosphate (S1P) is a novel fibrotic mediator in the eye. *Exp. Eye Res.* **87:** 367–375.
57. Berdyshev, E. V., I. Gorshkova, A. Skobeleva, R. Bittman, X. Lu, S. M. Dudek, T. Mirzapoiazova, J. G. Garcia, and V. Natarajan. 2009. FTY720 inhibits ceramide synthases and up-regulates dihydrosphingosine 1-phosphate formation in human lung endothelial cells. *J. Biol. Chem.* **284:** 5467–5477.
58. Lahiri, S., H. Park, E. L. Laviad, X. Lu, R. Bittman, and A. H. Futerman. 2009. Ceramide synthesis is modulated by the sphingosine analog FTY720 via a mixture of uncompetitive and noncompetitive inhibition in an acyl-CoA chain length-dependent manner. *J. Biol. Chem.* **284:** 16090–16098.
59. Schiffmann, S., D. Hartmann, S. Fuchs, K. Birod, N. Ferreiros, Y. Schreiber, A. Zivkovic, G. Geisslinger, S. Grosch, and H. Stark. 2012. Inhibitors of specific ceramide synthases. *Biochimie.* **94:** 558–565.
60. Mullen, T. D., Y. A. Hannun, and L. M. Obeid. 2012. Ceramide synthases at the centre of sphingolipid metabolism and biology. *Biochem. J.* **441:** 789–802.
61. Grösch, S., S. Schiffmann, and G. Geisslinger. 2012. Chain length-specific properties of ceramides. *Prog. Lipid Res.* **51:** 50–62.
62. Stiban, J., R. Tidhar, and A. H. Futerman. 2010. Ceramide synthases: roles in cell physiology and signaling. *Adv. Exp. Med. Biol.* **688:** 60–71.
63. Levy, M., and A. H. Futerman. 2010. Mammalian ceramide synthases. *IUBMB Life.* **62:** 347–356.
64. Hartmann, D., J. Lucks, S. Fuchs, S. Schiffmann, Y. Schreiber, N. Ferreiros, J. Merkens, R. Marschalek, G. Geisslinger, and S. Grosch. 2012. Long chain ceramides and very long chain ceramides have opposite effects on human breast and colon cancer cell growth. *Int. J. Biochem. Cell Biol.* **44:** 620–628.
65. Seumois, G., M. Fillet, L. Gillet, C. Faccinetto, C. Desmet, C. Francois, B. Dewals, C. Oury, A. Vanderplasschen, P. Lekeux, et al. 2007. De novo C16- and C24-ceramide generation contributes to spontaneous neutrophil apoptosis. *J. Leukoc. Biol.* **81:** 1477–1486.

66. Katritch, V., V. Cherezov, and R. C. Stevens. 2013. Structure-function of the G protein-coupled receptor superfamily. *Annu. Rev. Pharmacol. Toxicol.* **53:** 531–556.
67. Takuwa, N., S. Ohkura, S. Takashima, K. Ohtani, Y. Okamoto, T. Tanaka, K. Hirano, S. Usui, F. Wang, W. Du, et al. 2010. S1P3-mediated cardiac fibrosis in sphingosine kinase 1 transgenic mice involves reactive oxygen species. *Cardiovasc. Res.* **85:** 484–493.
68. Vogel, C., and E. M. Marcotte. 2012. Insights into the regulation of protein abundance from proteomic and transcriptomic analyses. *Nat. Rev. Genet.* **13:** 227–232.
69. de Sousa Abreu, R., L. O. Penalva, E. M. Marcotte, and C. Vogel. 2009. Global signatures of protein and mRNA expression levels. *Mol. Biosyst.* **5:** 1512–1526.
70. Maier, T., M. Guell, and L. Serrano. 2009. Correlation of mRNA and protein in complex biological samples. *FEBS Lett.* **583:** 3966–3973.
71. Lundberg, E., L. Fagerberg, D. Klevebring, I. Matic, T. Geiger, J. Cox, C. Algenas, J. Lundeberg, M. Mann, and M. Uhlen. 2010. Defining the transcriptome and proteome in three functionally different human cell lines. *Mol. Syst. Biol.* **6:** 450.